

LOGANATHAN
GOKULANATHAN¹
JEGAN ANNAMALAI²

Department of Mechanical
Engineering, Sona College of
Technology, Salem, Tamil Nadu,
India

AVS College of Technology,
Salem

SCIENTIFIC PAPER

UDC 544.6:669.24.0171.018

EXPERIMENTAL INVESTIGATION OF MICRO-ECM ON MONEL 400 ALLOY USING PARTICLES MIXED ELECTROLYTE

Article Highlights

- The micro-holes were fabricated over the MONEL 400 alloy
- The various electrolytes used here are MGAE, MPME, and CPME
- The parameters are electrolyte type, concentration, machining voltage, and duty cycle
- The results are optimized using MOORA and VIKOR techniques
- The best parameter for machining is 28 g/l of electrolyte, 11V machining voltage, and 50% duty cycle

Abstract

The machining of extremely hard material in conventional machining requires high energy. Therefore stress-free, burr-free, and high-accuracy machining technique like Electro Chemical Micro Machining (ECMM) with extra features is recommended. To improve efficiency, various electrolytes such as Magnet Associated Electrolytes (MGAE), Metal Particle Mixed Electrolytes (MPME), and Carbon Pellets Mixed Electrolytes (CPME) are employed. The micro-holes were drilled over the work material MONEL 400 alloy. The parameters for the studies are electrolyte type, concentration (g/l), machining voltage (V), and duty cycle (%). The responses of ECMM are estimated through material removal rate (MRR) in $\mu\text{m}/\text{sec}$ and overcut in μm . The results are optimized using Multi-objective optimization based on ratio analysis (MOORA) and VlseKriterijumska Optimizacija I Kompromisno Resenje (VIKOR). Both techniques produce the same optimal parameter, 18th experiment CPME, 50% duty cycle, 11 V machining voltage, and 28 g/l electrolyte concentration. It is the best optimal parameter solution for machining. According to the ANOVA table of both, the type of electrolyte plays a 62.6% and 60.37% contribution, respectively, to machining performance. Furthermore, the scanning electron microscope (SEM) image analysis perused on the micro holes to extend the effect of different electrolytes on machining surfaces.

Keywords: carbon pellets, MOORA, VIKOR, ECMM, metal particles, magnet.

ECMM creates numerous applications in different manufacturing sectors, such as medical, electronics, automobiles, and microelectromechanical systems. The machining of micro features in all kinds of

components is essential nowadays. Therefore, this paper mainly focuses on fabricating micro holes via the ECMM process [1]. The precision of micro-hole and machining performance of ECMM is acquired based on various factors such as electrical, nature of electrolyte, electrode, and adoption of the new technique. Also, it is mandatory in the fast-developing and challenging manufacturing sector to suppress the irregularity of machining and improve the machining performance simultaneously [2]. In line up with that, to improve micro-hole accuracy and machining performance, various research attempts are made by researchers worldwide. Therefore, Singh *et al.* [3] conducted experiments in the electrochemical discharge machin-

Correspondence: L. Gokulanathan, Department of Mechanical Engineering, Sona College of Technology, Salem, Tamil Nadu, India -636005.

E-mail: lgokulanathan@gmail.com

Paper received: 15 November, 2022

Paper revised: 19 May, 2023

Paper accepted: 21 June, 2023

<https://doi.org/10.2298/CICEQ221115013G>

ing process with multiple tooltip electrodes to investigate the effect of electrical frequency and duty cycle. They noted nonhomogeneous tool wear on the electrode due to the pulse variations in the sulfuric acid electrolyte. The frequency of 50 kHz is optimal for a better uniform machining rate and surface finish. Zhao *et al.* [4] conducted the experiment in ECMM with a curved voltage signal to improve the machining accuracy and derived a mathematical model. They noted the better agreement for curved pulse signals with experimental results. Also, they compared the results of pulse signals, such as rectangular and parabolic, to the experimental outputs and suggested parabolic signals. The parabolic signals diminish the machining gap ten times less, contributing to a better surface finish. Sharma *et al.* [5] investigated the effect of pulsed current between the tool and electrode and noted the suitable current distributions technique for the ECM process using simulation and experimental. The waveforms such as rectangular, sinusoidal, and triangular are employed in experimentations. They suggested that triangular waveforms produce a better surface finish and two times better machining rate than the normal waveforms. Panda *et al.* [6] employed the sulfuric acid electrolyte with rectangular electric pulses in ECMM of titanium alloy. They noted that machining voltage 13V–17 V produces better MRR with short pulses. Also, the taper of hole and overcut are reduced by around 83.99% and 51.39%, respectively, with this short pulse power supply. VinodKumar *et al.* [7] studied the ECMM performance with metal particles of copper mixed electrolyte on SS 316 work metal using the citric acid electrolyte. In addition, they employed the stirring mechanism to accelerate the movement of the ions in the electrolyte. They noted that employing an additional mechanism induces the unwanted surface finish due to the excess migration of electrons. Gokulanathan *et al.* [8] conducted experiments in ECMM on Monel 400 alloy with a pulsed air supply system to understand the effect of pulsed air suspension on machining performance. They noted that the micro stirring effect increases the electron's movement and leads to a better machining rate. Also, optimization techniques such as TOPSIS and COPRAS methods are employed to identify the optimal parameter solution. Kumar *et al.* [9] tried various organic electrolytes to study the machining performance of ECMM on SS 316 material. The electrolytes such as citric acid, tartaric, and mixed organic acid (citric acid and tartaric) in equal proportion are employed for the experiment. They noted that overcut of micro-hole was reduced by around 170% with tartaric acid, and MRR increased to 110% with mixed acid electrolyte. Also, the organic acids note very few surface irregularities over the work material. Arul *et*

al. [10] employed the aluminum composite electrode in the ECMM process to investigate surface accuracies. The square micro-hole is fabricated using a composite electrode, and the edges of the micro-hole are obtained neatly due to the uniform current distribution. Also, they noted that 43% improved over cut and 70% higher MRR with composite electrode than SS tool electrode. Vats *et al.* [11] fabricated the high-aspect micro holes using a hollow tube electrode through the ECMM process on nickel-based Inconel alloy. They noted lesser stray cuts and uniform current distribution in the machining zone. The inter-electrode gap provides a better way to dispel the dissolved parts from the machining zone because of the hollow tool. The surface roughness of the micro-hole significantly improved by around 20% with a hollow tube electrode than a normal tool. Rajkeerthi *et al.* [12] conducted experiments using a hollow taper tool and cylindrical hollow tool in the ECMM process on nickel-based superalloy. They noted that the tapered hollow tool reduces the over-cut by up to 2.5% and increases the MRR by around 24% more than normal cylindrical hollow tools. Thanigaivelan *et al.* [16] tried different mixed electrolytes, such as plain sodium nitrate, plain sodium chloride, and mixed sodium nitrate and sodium chloride, for the ECMM process. They noted significant improvement in MRR due to the solution's accelerated electron movements. Wang *et al.* [17] used acoustic emission to improve the ECM process's machining performance. It has been noted that two times better overcut with this mechanism, and ultrasonic vibrations dispel the machined products from the machining zone quickly, leading to a better surface finish. Liu *et al.* [18] tried the heat-treated copper electrodes in the ECMM process using sodium nitrate electrolyte. They mentioned that lesser overcut was obtained with heat-treated electrodes than with normal electrodes due to the high electrical conductivity of the electrode. Zhan *et al.* [19] investigated the machining performance of ECM with a gas-assisted tool electrode. The assistance of gas surrounding the electrode act as insulation, preventing unwanted material removal and causing lesser overcut. The literature discussed above clearly notes that many researchers employed electrolytes and electrodes to enhance ECMM performance. The electrolytes are fabricated by mixing magnets, metal powder, and carbon pellets in different ranges to enhance the machining performance. The results of these electrolytes, such as MGAE, MPME, and CPME, are compared. Also, these mixing elements are successfully employed in other sectors such as electrical batteries, metal coating, electrical discharge machining, etc. [20,21,22]. Although magnets and metal mixed studies exist in the literature, it is not adequate data for commercial execution, and carbon pellets are employed in electrolytes for the first time in

this attempt. Carbon materials naturally stimulate electrolyte conductance when mixed in water. Also, the process parameters are optimized through the most prominent optimization techniques, such as MOORA and VIKOR methods. Furthermore, SEM figures analysis is carried out to show the performance of the machining process, and microholes are affected by various electrolytes. Matsuzawa *et al.* [28] ECM can be performed on any workpiece regardless of its hardness. However, the machining direction is confined to the gravitational direction because ECM uses electrolytes. The electrolyte is frozen using a Peltier device. This method uses the principle of the Peltier device to freeze the electrolyte and seal it in an electrode. Wang *et al.* [29] Electrochemical machining (ECM) is widely employed to machine tough materials. A non-conductive solid porous ball is used as an electrolyte absorption material in ECM. Ge *et al.* [30] Casing parts are considered key components of aero-engines. Most casing parts are attached to convex structures of different shapes, whose heights range from hundreds of microns to tens of millimeters. It indicates that the back-pressure method is suitable and effective for the electrochemical machining of highly convex structures with blocky electrodes. From the literature mentioned above section, the research gap is found that pulsed air supply for this electrochemical micromachining is proposed in this work along with the many different electrolytes like MGAE, MPME, and CPME going to be tested in the proposed methodology.

MATERIAL AND METHODS

For the experiment shown in Fig. 1, an ECMM setup that was autonomously manufactured was used. The experimental setup included various sub-

components, a voltage rectifier, a tool transmission system, and an electrolyte recycling supply arrangement. Considering the demand for Monel 400 in various fields, this paper employed a 0.8 mm thick plate as work material. SS material is considered for all three electrodes with a length of 4.5 cm and a diameter of 500 μm . The pulsed air supply system is employed in all experiments. The experiments are planned with different methods of electrolytes. Hence, commercially available ferrite (Fe_2O_3) permanent magnets (40 mm x 20 mm x 5 mm in size) are fixed on the electrolyte tank for both sides of the wall and considered MGAE. The experimental setup and MGAE method are presented in Fig. 1. The activated carbon pellets in sizes of 2 mm dia, 5 mm length, and 25 grams are mixed with the electrolyte. Activated carbon pellets exist commercially, and this electrolyte is termed CPME. The 25-gram Nano-sized zinc metal particle is mixed with the standard electrolyte, MPME [23]. The total machining time is noted to evaluate the machining rate. The differences in diameter between the tool and micro hole are measured using an optical microscope to find the overcut of the micro-hole. The hole formation was noted by the witness of hydrogen bubbles beneath the micro-hole. The range of machining parameters and the design of the experiment are presented in Tables 1 and 2, respectively.

Table 1. Machining factors and their levels.

Machining factors	Levels
Type of Electrolyte	MGAE, MPME, CPME
Electrolyte Concentration in g/l	24, 26, 28
Machining voltage in v	9, 11, 13
Duty Cycle in %	50, 75, 90

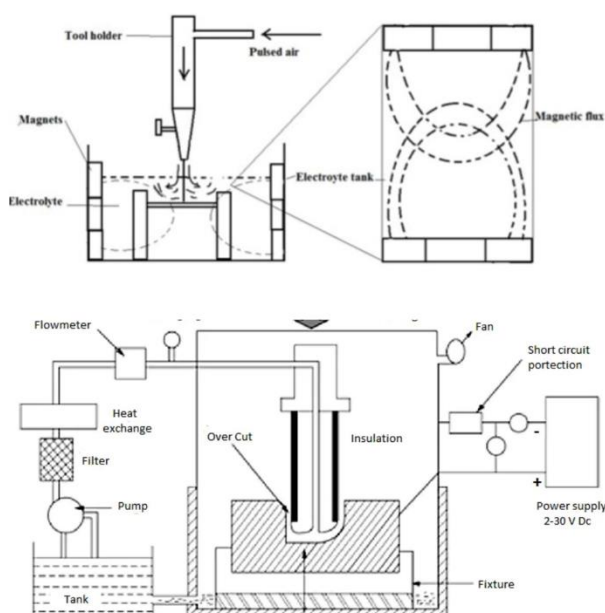


Figure 1. Experimental setup (a) Magnet-associated electrolyte (b) Carbon pellets.

Table 2. Design of experiments and outcomes.

Ex. No	Type of Electrolyte	Elet. Con. in g/l	Mach. Volt in V	Du. Cycle in %	MR in $\mu\text{m} / \text{sec}$	Overcut in μm
1	MGAE	24	9	50	0.6197	152.05
2	MGAE	26	11	75	0.7279	210.04
3	MGAE	28	13	90	0.8070	201.66
4	MPME	24	9	75	0.4655	100.43
5	MPME	26	11	90	0.8514	126.85
6	MPME	28	13	50	0.9296	186.86
7	CPME	24	11	50	0.8556	110.84
8	CPME	26	13	75	0.7365	124.45
9	CPME	28	9	90	0.8863	116.04
10	MGAE	24	13	90	0.6089	135.84
11	MGAE	26	9	50	0.8090	187.85
12	MGAE	28	11	75	0.7274	205.58
13	MPME	24	11	90	0.5046	96.68
14	MPME	26	13	50	0.6637	102.77
15	MPME	28	9	75	0.8573	182.46
16	CPME	24	13	75	0.6987	104.55
17	CPME	26	9	90	0.8183	114.47
18	CPME	28	11	50	0.8491	100.87

OPTIMIZATION

VIKOR

VIKOR is one of the most robust and reliable techniques for multi-criteria optimization to find the optimal parameter solution. The following steps are followed to evaluate the best machining combination [24] which are;

Step 1. Different dimensioned values are converted into single form by normalization using Eqs. 1 and 2. Also, a positive sign was assigned for MR, and a negative sign was assigned for minimization.

$$S_m = \begin{bmatrix} T_{11} & T_{12} & T_{13} & T_{1n} \\ T_{21} & T_{22} & T_{23} & T_{2n} \\ T_{31} & T_{32} & T_{33} & T_{3n} \\ \vdots & \vdots & \vdots & \vdots \\ T_{m1} & T_{m2} & T_{m3} & T_{mn} \end{bmatrix} \quad (1)$$

$$t_{ij} = \frac{T_{ij}}{\sqrt{\sum_{i=1}^m T_{ij}^2}}, \quad j = 1, 2, \dots, n. \quad (2)$$

Step 2. The uppermost and least values are noted from the decision matrix to find the C_i and D_i using Eqs. 3 and 4, respectively.

$$C_i = \sum_{j=1}^n R_j [(b_j)_{\max} - (b_j)] / [(b)_{\max} - (b)_{\min}] \quad (3)$$

$$D_i = \text{Max}^n \left\{ \frac{[R_j (b)_{\max} - (b_j)]}{[(b)_{\max} - (b)_{\min}]} \right\}, \quad j = 1, 2, \dots, n. \quad (4)$$

where R_j is the weighted value (equal weight assigned).

Step 3- P_i values are estimated through C_i and D_i

using Eq. 5.

$$P_i = R \frac{C_i - C_{i-\min}}{C_{i-\max} - C_{i-\min}} + (1-R) \frac{D_i - D_{i-\min}}{D_{i-\max} - D_{i-\min}} \quad (5)$$

Step 4. Lowest P_i values are considered the best solution, and others are followed in the rank order.

MOORA

MOORA is another excellent and straightforward technique to identify the suitable parameter solution from a certain number of experiments [25].

Step 1. Normalization is carried out by the Eqs. 1 and 2.

Step 2. Values are added for higher needs and have to subtract for lesser needs using Eq. 6.

$$J_i = \sum_{j=1}^g M_j - \sum_{j=g+1}^n m_j \quad (6)$$

Step 4. Equal weights are assigned to all outputs, multiplied by w_j in the Eq. 7.

$$T_i = \sum_{j=1}^g w_j M_j - \sum_{j=g+1}^n w_j m_j, \quad j = 1, 2, \dots, n. \quad (7)$$

Finally, T_i values are graded, and higher values are ranked as one and termed as the best optimal combination.

RESULTS AND DISCUSSION

Influences of input parameters on overcut

The overcut of all input parameters is drawn as a graph and presented in Fig. 2. The data sets of the

graph are prepared according to the mean values of overcut. The graph infers that overcut increases when increasing input parameter ranges. Also, it indicates that MGAE produced the least overcut among the different electrolytes, and the highest overcut was found to be with the MPME. MGAE and CPME produce 35.08% and 11.61% lesser overcut, respectively, than MPME. In one of our previous experiments, plain air-assisted electrolyte [8] obtained 124.23 μm overcut for the first optimal combination, whereas, in the present study, the MGAE produces 111.87 μm overcut. This value is 9.9% lesser than the plain air-assisted electrolyte. Fig. 3a presents the SEM image of the micro-hole machined under the MGAE, which shows the precise circumference and micropores surface.

The use of magnets in the electrolyte induces magnetic flux pressure over the movement of the ions at the machining zone. Hence, continuous sludge removal is carried between the tool and electrode, which ensures the unwanted electric current conduct among electrolytes. Also, the uniform electric current flow passage settled among the movement of the electron, as explained in Fig. 1. This phenomenon is caused for the lesser overcut in the MGAE. Also, in MGAE, additional substances are not mixed, which enables the homogeneous current conductivity and causes the best surface finish and lesser over-cut. The

CPME produces 152.38 μm overcut. The second least overcut in the experiment. SEM images of a micro hole machined with CPME and MPME are presented in Fig. 3b and Fig. 3c. Carbon particles conduct electricity smoothly and uniformly by their soft crystallographic nature [20].

On the other hand, metal particles create a strong conduction bridge in the electrolyte which induces the turbulent ion movement [26], which causes the excess material removal and leads to a lesser overcut with CPME than MPME. The case of other machining parameters produces the magnified overcut when increasing the levels. It is obvious that the dissolution range increase or decreases based on the input ranges supplied to the machining zone.

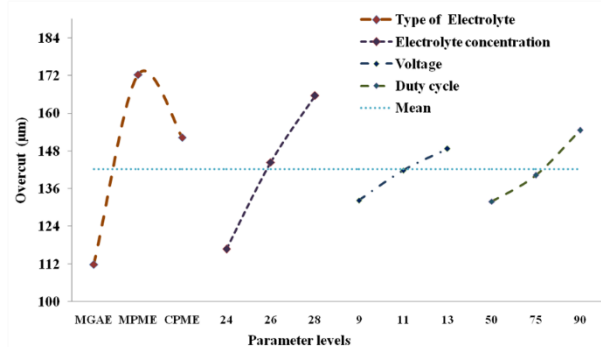


Figure 2. Influences of different parameters on overcut.

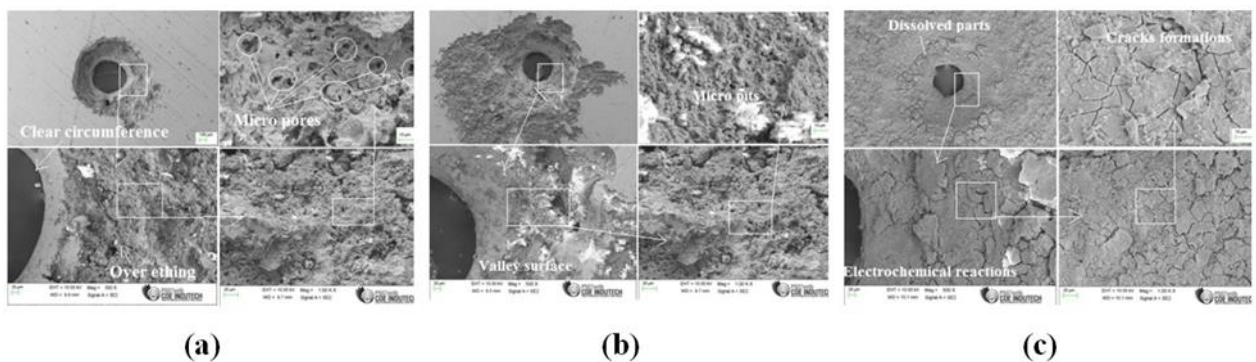


Figure 3. SEM image of micro holes (a) MGAE (b) CPME (c) MPME.

Influences of input parameters on MRR

The influences of various input parameters on MRR and its values are presented as a graph in Fig. 4. The graph indicates that a range of input parameters increases the MRR. Among those uses, different electrolytes contribute more MRR than other parameters. Based on that, MPME produces the highest MRR among different electrolytes and the lowest MRR obtained with MGAE. The MPME and CPME produce 27.92% and 17.93% higher MRR, respectively, than the MGAE. Although, the MGAE produces 6.57% higher MRR than the literature [8], which is obtained for the optimal solution. The primary

cause for the highest MRR with MPME is Nano metal particles. Since the Nano metal particle creates the connection pathway for the vibrant electrons movement in the electrolyte by its range of size, this character of electrolyte implies faster ion migration, leading to the highest MRR than others. The CPME produces the second-highest MRR. Since the carbon pellets post up the conductivity of the electrolyte due to the series connections, it acts like a storage barrier that transmits the electric energy to the electrolyte between the pulses on time [20]. This phenomenon of carbon-mixed electrolytes causes a higher MRR. Also, the graph shows the increasing trend concerning all ranges of

levels. It is because the high state of the machining parameter enables rapid ion oscillation. Also, in the higher range of machining, the dissolved particle of the work plate merges with the electrolyte and induces electric conductivity among the electrolyte.

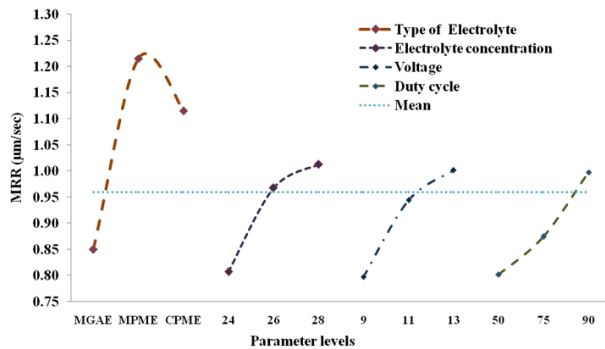


Figure 4. Influences of different parameters on MRR.

Estimation of optimal combinations

VIKOR

The perfect parameter value is determined by the VIKOR method [24]. Equal weights are provided to the output responses. The VIKOR compromised values are ranked as lowest is best and furthest is the worst solution, presented in Table 3a. Based on the table, the least compromised value was obtained in experiment no 18. Hence, the 18th experiment parameter solution of CPME, electrolyte level of 28 g/l, machining voltage of 11 V, and duty cycle of 50% is considered a suitable parameter solution for machining. Experiments 9 and 7 show the next ranking orders and are considered the 2nd and 3rd optimal combinations for machining.

ANOVA table estimated the preference values used to investigate the machining performance statically [27]. The VIKOR study involves the ANOVA values to find the most critical parameter in machining, presented in Table 4a. Based on the table, electrolyte type plays a 62.6% contribution to machining performance. The machining voltage and duty cycle contribute 12.63% and 12.38%, respectively, to the performance. The very least contribution was obtained with the electrolyte concentration factor.

MOORA

MOORA method estimates the suitable parameter combination for ECMM with different electrolytes and machining parameters [27]. The obtained MOORA values and their ranking are presented in Table 3b. The Eqs. 1, 2, 6 and 7 are used for the MOORA values. An equal weight of 0.5 is assigned for both output values. The uppermost MOORA value is taken as an optimal solution and termed first grade to obtain a better machining outcome.

Table 3. a) Ranking of responses in VIKOR; b) MOORA and its ranking.

Ex. No	R_i	S_i	VIKOR (T_i)	Rank
1	0.5781	0.6749	0.7903	15
2	0.7173	0.7879	1.0000	18
3	0.5952	0.6892	0.8165	16
4	0.5165	0.6226	0.6956	12
5	0.2174	0.3346	0.2068	5
6	0.3978	0.5162	0.5083	9
7	0.1423	0.2469	0.0710	3
8	0.3306	0.4520	0.3989	8
9	0.1321	0.2341	0.0519	2
10	0.5183	0.6241	0.6983	13
11	0.5321	0.6360	0.7198	14
12	0.6981	0.7728	0.9715	17
13	0.4579	0.5710	0.6039	11
14	0.3133	0.4350	0.3703	7
15	0.4563	0.5696	0.6015	10
16	0.2835	0.4049	0.3205	6
17	0.1984	0.3134	0.1733	4
18	0.1052	0.1989	0.0000	1

Table 3b.

Ex. No	Normalized Responses		MOORA value (Y_i)	Rank
	MR	OC		
1	0.1932	0.2423	0.4433	14
2	0.2269	0.3348	0.2995	18
3	0.2515	0.3214	0.3846	16
4	0.1451	0.1601	0.5468	10
5	0.2654	0.2022	0.7685	5
6	0.2898	0.2978	0.5095	12
7	0.2667	0.1767	0.8607	2
8	0.2295	0.1984	0.6822	8
9	0.2762	0.1850	0.8553	3
10	0.1898	0.2165	0.5175	11
11	0.2521	0.2994	0.4289	15
12	0.2267	0.3277	0.3074	17
13	0.1573	0.1541	0.5775	9
14	0.2069	0.1638	0.6854	7
15	0.2672	0.2908	0.4836	13
16	0.2178	0.1666	0.7148	6
17	0.2551	0.1824	0.8074	4
18	0.2646	0.1608	0.8904	1

In line with that, the 18th experiment carried the farthest MOORA grade, 0.8904. 18th experimental run parameter combinations present 0.8491 $\mu\text{m}/\text{sec}$ MRR and 100.87 μm overcut. Hence, based on the MOORA method, these experiment parameter characteristics: CPME, 11 V machining voltage, 28 g/l electrolyte concentration, and 50% duty cycle is considered suitable parameter solution for machining. Also, experiments 7th and 9th are optimal parameter combinations for better outcome machining.

Table 4. a) ANOVA of VIKOR; b) ANOVA for MOORA.

Machining parameter	DOF	SS	MS	F	% OF CON
Type of electrolyte	2	0.3920	0.196	39.357	62.81
Electrolyte concentration	2	0.0406	0.0203	4.0779	6.51
Machining voltage	2	0.0788	0.0394	7.9153	12.63
Duty cycle	2	0.0773	0.0386	7.7598	12.38
Error	9	0.0448	0.005		5.66
Total	17	0.6336	0.0373		100

Table 4b.

Machining parameter	DOF	SS	MS	F	% OF CON
Type of electrolyte	2	1.0206	0.5103	41.562	60.37
Electrolyte concentration	2	0.1987	0.0993	8.0899	11.75
Machining voltage	2	0.1206	0.0603	4.9108	7.13
frequency	2	0.2450	0.1225	9.9773	14.49
Error	9	0.1105	0.0123		6.26
Total	17	1.6953	0.0997		100

CONCLUSION

The primary objective of this investigation is to emphasize the machining process of ECMM using different inorganic materials mixed electrolytes along with a pulsed air supply system for Monel 400 alloy. The results of the machining process are optimized through VIKOR and MOORA methods.

MPME produces the highest MRR and lowest MRR obtained with MGAE. MPME and CPME produce 27.92% and 17.93% higher MRR, respectively, than the MGAE.

MGAE produces the least overcut and highest overcut found in MPME. MGAE and CPME produce 35.08% and 11.61% lesser overcut, respectively, than MPME.

CPME produces 152.38 μm overcut, the second least overcut in the experiment. Carbon particles conduct electricity smoother and more uniformly through their soft crystallographic nature.

Both optimization techniques, VIKOR and MOORA, produce the same optimal parameter for machining as the 18th experiment parameter solution, CPME 50% duty cycle, an 11 V machining voltage, and a 28 g/l electrolyte concentration.

SEM image analysis extends the understanding of the effect of different electrolytes on the micro holes, which presents the over-etching surface near the micro holes due to the synergistic effect of electrochemical reactions.

REFERENCES

- [1] T.S. Srivatsan, T.S. Sudarshan, K. Manigandan, Textbook of Manufacturing Techniques for Materials: Engineering and Engineered (1st ed.), CRC Press, Boca Raton (2018), p. 814. <https://doi.org/10.1201/b22313>.
- [2] M. Soundarrajan, R. Thanigaivelan, Russ. J. Electrochem. 57 (2021) 172–182. <https://doi.org/10.1134/S1023193521020117>.
- [3] T. Singh, D.K. Mishra, P. Dixit, J. Appl. Electrochem. 52 (2022) 667–682. <https://doi.org/10.1007/s10800-021-01662-x>.
- [4] C. Zhao, T. Huang, J. Wang, L. Xu, Int. J. Adv. Manuf. Technol. 121 (2022) 3067–3078. <https://doi.org/10.1007/s00170-022-09482-9>.
- [5] V. Sharma, P. Gupta, J. Ramkumar, J. Manuf. Processes. 75 (2022) 110–124. <https://doi.org/10.1016/j.jmapro.2022.01.006>.
- [6] H. S. Panda, K. Mishra, B. Bhattacharyya, J. Electrochem. Soc. 169 (2022). <https://doi.org/10.1149/1945-7111/ac6e8e>.
- [7] J.R. Vinodkumar, R. Thanigaivelan, M. Soundarrajan, Mater. Manuf. Processes. (2022) 1–14. <https://doi.org/10.1080/10426914.2022.2030874>.
- [8] L. Gokulanathan, A. Jegan, Int. J. Electrochem. Sci. 17 (2022) 2. <https://doi.org/10.20964/2022.08.55>.
- [9] J.R.K.V. Kumar, R. Thanigaivelan, M. Soundarrajan, Chem. Ind. Chem. Eng. Q. 28(4) (2022) 329–337. <https://doi.org/10.2298/CICEQ211204007V>.
- [10] T.G. Arul, V. Perumal, R. Thanigaivelan, Chem. Ind. Chem. Eng. Q. 28 (2022) 247–253. <https://doi.org/10.2298/CICEQ210501036A>.
- [11] A. Vats, A. Dvivedi, P. Kumar, Mater. Manuf. Processes. 36 (2021) 677–692. <https://doi.org/10.1080/10426914.2020.1866189>.
- [12] E. Rajkeerthi, P. Hariharan, N. Pradeep, Mater. Manuf. Processes. 36 (2021) 488–500. <https://doi.org/10.1080/10426914.2020.1843672>.
- [13] M. Soundarrajan, R. Thanigaivelan, S. Maniraj, In Advances in Industrial Automation and Smart Manufacturing, Springer, Singapore (2021), p. 367–376.

- https://doi.org/10.1007/978-981-15-4739-3_30
- [14] R. Shanmugam, M. Ramoni, G. Thangamani, M. Thangaraj, *Metals*. 11 (2021) 778. <https://doi.org/10.3390/met11050778>.
- [15] M. Soundarrajan, R. Thanigaivelan, *Mater. Manuf. Processes*. 35 (2020) 775–782. <https://doi.org/10.1080/10426914.2020.1740252>.
- [16] V. Subburam, S. Ramesh, R.M. Arunachalam, R. Thanigaivelan, In *Proceedings of the second international conference on advances in materials processing and characterisation-AMPC* (2013), p. 799–806.
- [17] G. Wang, Y. Zhang, H. Li, J. Tang, *Materials*. 13 (2020) 5780. <https://doi.org/10.3390/ma13245780>.
- [18] S. Liu, T. Geethapriyan, T. Muthuramalingam, R. Shanmugam, Ramoni, *Arch. Civ. Mech. Eng.* 22 (2022) 1–15. <https://doi.org/10.1007/s43452-022-00478-6>.
- [19] S. Zhan, Y. Zhao, *J. Mater. Process. Technol.* 291 (2021) 117049. <https://doi.org/10.1016/j.jmatprotec.2021.117049>.
- [20] M. Deraman, S. Zakaria, R. Omar, A.A. Aziz, *Jpn. J. Appl. Phys.* 39 (2000) L1236. <https://doi.org/10.1143/JJAP.39.L1236>.
- [21] P. Kapitza, *Proc. R. Soc. London, Ser. A*, 123 (1929) 292–341. <https://doi.org/10.1098/rspa.1929.0072>.
- [22] Jadidi, R.B. Azhiri, R. Teimouri, *Int. J. Lightweight Mater. Manuf.* 3 (2020) 265–276. <https://doi.org/10.1016/j.ijlmm.2020.02.004>.
- [23] R. Kumar, R. Thanigaivelan, G.K. Rajanikant, T. Jagadeesha, J. Das, *J. Aust. Ceram. Soc.* 57 (2021) 107–116. <https://doi.org/10.1007/s41779-020-00517-6>.
- [24] Jahan, F. Mustapha, M. Y. Ismail, S. M. Sapuan, M. Bahraminasab, *Mater. Des.* 32 (2011) 1215–1221. <https://doi.org/10.1016/j.matdes.2010.10.015>.
- [25] M. Soundarrajan, R. Thanigaivelan, In *Advances in Micro and Nano Manufacturing and Surface Engineering*, Springer, Singapore (2019), p. 423–434.
- [26] Pramanik, *Int. J. Mach. Tools Manuf.* 86 (2014) 44–61. <https://doi.org/10.1016/j.ijmactools.2014.07.00>.
- [27] H. Majumder, K. Maity, *Measurement*. 118 (2018) 1–13. <https://doi.org/10.1016/j.measurement.2018.01.003>.
- [28] K. Matsuzawa, S. Oka, M. Uchiyama, *Procedia CIRP*. 113 (2022) 483–487. <https://doi.org/10.1016/j.procir.2022.09.204>.
- [29] J. Wang, W. Natsu, *Precis. Eng.* 77 (2022) 307–319. <https://doi.org/10.1016/j.precisioneng.2022.06.012>.
- [30] Z. Ge, W. Chen, *Chin. J. Mech. Eng.* 35 (2022) 98. <https://doi.org/10.1186/s10033-022-00752-x>.

LOGANATHAN
GOKULANATHAN¹
JEGAN ANNAMALAI²

Department of Mechanical
Engineering, Sona College of
Technology, Salem, Tamil Nadu,
India

AVS College of Technology,
Salem

NAUČNI RAD

EKSPERIMENTALNO ISTRAŽIVANJE ELEKTROHEMIJSKE MIKRO OBRADNE LEGURE MONEL 400 KORIŠĆENJEM ELEKTROLITA SA ČESTICAMA

Konvencionalna mašinska obrada izuzetno tvrdog materijala zahteva veliku energiju. Zbog toga se preporučuje tehnika obrade bez naprezanja, bez ivica i visoke preciznosti, kao što je elektrohemijaska mikro obrada (sa dodatnim funkcijama). Da bi se poboljšala efikasnost, koriste se različiti elektroliti, kao što su elektroliti sa magnetima, elektroliti sa metalnim česticama i elektroliti sa ugljeničnim peletama (CPME). Mikro-rupe su izbušene u radnom materijalu, tj. leguri MONEL 400. Parametri istraživanja su tip elektrolita, koncentracija (g/l), napon obrade (V) i radni ciklus (%). Rezultati elektrohemijske mikro obrade se procenjuju putem brzine uklanjanja materijala u $\mu\text{m}/\text{sec}$ i prekoračenja u μm . Rezultati su optimizovani korišćenjem višeciljne optimizacije zasnovane na analizi odnosa i višekriterijumske optimizacije i kompromisnog rešenja. Obe tehnike određuju iste optimalne parametre: 18ti eksperiment CPME, radni ciklus 50%, napon obrade 11 V i koncentracija elektrolita 28 g/l. To je najbolje optimalno parametarsko rešenje za mašinsku obradu. ANOVA je pokazala da oba tipa elektrolita doprinose performansama obrade sa 62,6% i 60,37%. Štaviše, skenirajućim elektronskim mikroskopom pregledane su mikro rupe da bi se proširio efekat različitih elektrolita na obrađene površine.

Ključne reči: ugljenične pelete, višeciljna optimizacija zasnovana na analizi odnosa, višekriterijumska optimizacija i kompromisno rešenje, elektrohemijaska mikro obrada, metalne čestice, magnet.